

Extension Effects on the Phase Structure of Polyester-Polyurethane Elastomer Yarns by ^{13}C MAS-NMR Spectroscopy

Jie-Feng Shi, L. Charles Dickinson,* and James C. W. Chien*

Department of Polymer Science and Engineering, University of Massachusetts, Amherst, Massachusetts 01003

Received April 4, 1991; Revised Manuscript Received January 7, 1992

ABSTRACT: ^{13}C MAS-NMR spectra have been measured as a function of extension on a segmented polyester-polyurethane elastomer (Lycra 128) by both cross-polarization and Bloch decay techniques. A sample spooling technique was developed for magic angle spinning of elastomers under extension. Analysis cross-polarization dynamics allows semiquantitative analysis of three soft segment motional regimes over the full extension range: bulk, strained, and crystalline. Moderate extension had a significant effect on the proton spin-lattice relaxation but not on the carbon spin-lattice relaxation and proton rotating frame spin-lattice relaxation.

Thermoplastic elastomers based polyurethane segmented copolymers were developed over 25 years ago. These polymers have enjoyed great commercial success compared to vulcanized or thermoset rubbers because of their versatility in fabrication, especially in the formation of fine multifilament threads or yarns. Their molecular structures have been characterized principally by differential scanning calorimetry (DSC) and by X-ray crystallography,¹⁻³ which showed phase-separated "hard" and "soft" segment domains with the former acting as physical cross-links. A recent pair of papers relates X-ray, DSC, and mechanical measurements on these systems.^{4,5} The principal objective of this work was to use carbon-13 magic angle spinning nuclear magnetic resonance (^{13}C MAS-NMR) spectroscopy to observe some new structural details of these systems, particularly as regards the effect of extension on the structures of both the rigid domains and on the chain segments trapped in the soft domains. This paper reports such observations on a polyurethane-based elastomer with polyester soft segments. A companion paper⁶ reports results on the polyether-polyurethanes which exhibit strain-induced crystallization.

Experimental Section

Lycra 128 was obtained from E. I. DuPont and Co., Wilmington, Delaware. This material was manufactured from a macroglycolic polyester of molecular weight 3500 based on adipic acid, butanediol, and ethylene glycol. This macroglycol was end-reacted with excess 4,4'-methylenebis(phenyl isocyanate) (MDI) and chain-extended with ethylene glycol to a molecular weight of 50 000. The MDI plus ethylene glycol constituted nominally 15 wt % of the TPE. This material is referred to as PEsU to designate poly(ester-urethane).

Samples were received as approximately 500 denier yarns. (1 denier = 1 g/9000 m). In order to make observations on the hard segment regions and to have as narrow a line width as possible for the soft segments, we needed to spin an axially symmetric specimen in typical MAS fashion. Simply packing a rotor with even, short lengths of yarn does not give adequate spinning rates. We devised a method of spinning stretched MAS-NMR samples. Spool rods were cut on a lathe from $\frac{1}{4}$ -in. Delrin or KelF rod. The spool part of the rod was precisely cut to slip fit into the 6-mm-i.d. MAS rotor and to be of the correct length available between rotor end caps. The inner part of the spool which would hold the wound yarn was cut on a lathe to leave sufficient diameter remaining to support the spool under the stress of winding: 1.5 mm for Delrin, 2 mm for KelF. When the spool was cut from the original rod, an approximately 1.5-mm diameter of the outer ends of the spool was left uncut so that the spool was left well attached to the $\frac{1}{4}$ -in.-diameter rod. In order to wind samples

of constant elongation onto the spool a weight appropriate to give the desired elongation was attached to end of the yarn, the necessary length of unstretched yarn paid out, and the end attached to the spool with a minimum of cyanoacrylate glue. The yarn was then extended in the extreme case by ascending a stairwell, ca. 125 ft. high, so that the constant tension caused the weight to lift. At this point the rod end could be inserted into the chuck of a slow-speed electric motor to wind the yarn onto the spool. Some samples were wound by hand. Once wound, the end was attached with the same minimal glue and the spool was cut away from the larger rod with a razor. The wound spools fit smoothly into the Doty rotor and spun easily at 5 kHz, and wound samples could be stored and reused.

Samples are labeled by their extension ratio $\lambda = L/L_0$ where L_0 is the original length of the yarn. The nominal $\lambda = 1$ sample was actually stretched 5% in order to achieve smooth windings. One sample was stretched to $\lambda = 7$ and allowed to fully relax for 20 h before the spectrum was run. No further changes were seen in the NMR spectrum up to 10 days after stretching and this sample is referred to as "relaxed" or R.

NMR spectra were obtained at 50 MHz on an IBM-AF200 spectrometer fitted with an IBM Solids Accessory rack and Doty Scientific (Columbia, SC) multinuclear CP-MAS probe. Carbon and proton pulses were 5 μs (i.e. 50-kHz spin lock), and spinning was accomplished at or near 5 kHz. The two basic spin preparation pulse sequences used were cross-polarization (CP) and direct polarization (DP). CP included a $\pi/2$ proton pulse, followed by simultaneous pulses on the proton and carbon channels typically of length 2 ms and immediate subsequent observation under high-power decoupling. DP was a simple carbon $\pi/2$ pulse followed by decoupling during observation, that is, Bloch decay. Because CP requires dipolar coupling between the proton and carbon nuclei, it favors the observation rigid regions, DP will detect all carbon nuclei if sufficient time is allowed for the magnetization to return to equilibrium. Recycle times were 3 s except for the $T_1\rho$ experiment where they were 15 s.

We have adapted the dipolar dephasing technique of Lippa⁷ to discern types of rigid environment in our system. They devised this sequence to discern which peaks in a carbon spectrum belong to carbons which have attached protons. The essence of the sequence is a delay of 0-100 μs after the preparation pulses. A large dipolar interaction for carbons with attached protons causes spin-spin relaxation times dramatically shorter than those without attached protons use. We use the technique here to distinguish regions contributing to a given resonance position by the different effective spin-spin relaxation times associated with a given resonance. In our usage we expect motion to average the dipolar interaction for a given chemical moiety and if there are regions of different mobilities we will see different decay times, T_2^* . The pulse sequence simply adds a variable delay after the preparation pulse which allows decay of the transverse magnetization. Depending upon the mode of preparation of the spins,

the dipolar dephasing (DD) sequence is labeled DDCP or DDDP in accordance with the labeling above. A drawback of this is that the relative intensities of all the carbons are not reliably quantitative. Dephasing curves were fit with a simple sum-of-functions routine including both Gaussian and Lorentzian decays.

Spin-lattice relaxation times were measured by the π - τ - $\pi/2$ sequence, and in some cases the phase cycling of Torchia⁸ was used to eliminate the need to know the value of equilibrium magnetization. T_1^H and $T_{1\rho}^H$ were measured indirectly from the carbon intensity by the methods of Schaefer.⁹ For T_1^H a proton π - τ - $\pi/2$ and delay are performed prior to CP. Similarly, $T_{1\rho}^H$ was measured by varying the proton spin lock time prior to CP preparation and was calculated as previously described.¹⁰

Fitting relaxation data points to single- and double-exponential decays nominally allowed $\pm 10\%$ error. The data points for cross-polarization dynamics of carbon spectral intensity were fitted to two rising exponentials, $A_i \exp(-t/T_{CH,i})$, minus a falling exponential term, $(A_i + A_j) \exp(-t/T_1, \rho)$. Error estimation in these best fit parameters as given in the tables was based on the curvature of the χ^2 error surface at the minimum with respect to each parameter.¹¹ A 5% standard deviation was assumed for individual intensity measurements. As is evident from the small error values the χ^2 surface defines the fitted parameters well. Errors listed in the table are twice the calculated standard deviation from the curvature technique. Errors were calculated for each individual fitting χ^2 surface.

Results

Figure 1 shows the ^{13}C CP-MAS-NMR spectra at room temperature of PEsU samples for elongations of 1, 1.6, 3, and 7 and "relaxed" with the spins prepared by both DP and CP sequences. Peak assignments are listed in Table I. The two dramatic differences between DP and CP for the $\lambda = 1$ samples are high relative intensity of the 172.2 ppm carbonyl peak in the DP spectrum and the appearance of a range of aromatic peaks in the CP spectrum. (The large peak at 80 ppm is from the Delrin spool.) These effects are a function of the relative sensitivity of CP and DP. The aromatic region in the expanded scale (Figure 2) shows significant effects of extension on line shape and position for the hard segment domains.

Small intensity and line width changes can be seen with increased extension in Figure 1a,b. Because some of the peaks are unresolved or slightly overlapping we chose to describe the changes in shape by simply calculating the second moment of the line shape.¹² The results summarized in Table II clearly show a gradual increase in the second moment with extension from 1 to 3 and a dramatic increase at the near ultimate extension of the $\lambda = 7$ sample (fully extended). The fully extended sample upon relaxation does not fully recover the original second moment values of the unextended elastomer. The CP spectrum of the fully extended sample shows increased splitting of the CH_2O peaks near 62 ppm as well as a marked increase in the carbonyl relative intensity.

Relaxation time data for the elastomer at various extension values are given in Table III. Generally, $T_{1\rho}^H$ and T_1^C do not change with extension but T_1^H , T_{CH} , and T_2^* do show some sensitivity to extension before the major structural change at $\lambda = 7$. T_1^H shows the most consistent change with extension. The relaxed sample has some relaxation time values different from those of the unstretched sample. For the $\lambda = 7$ sample T_2^* and T_1^C are found to be multiphasic and the decay was resolved into two components. In the case of T_1^C the data were fit to two exponentials; for T_2^* the decay was best fitted to a sum of Lorentzian and Gaussian decays, as illustrated in Figure 3. The contribution of each component is listed in Table III and the analysis of both T_2^* and T_1^C give the same relative contribution of short and long components.

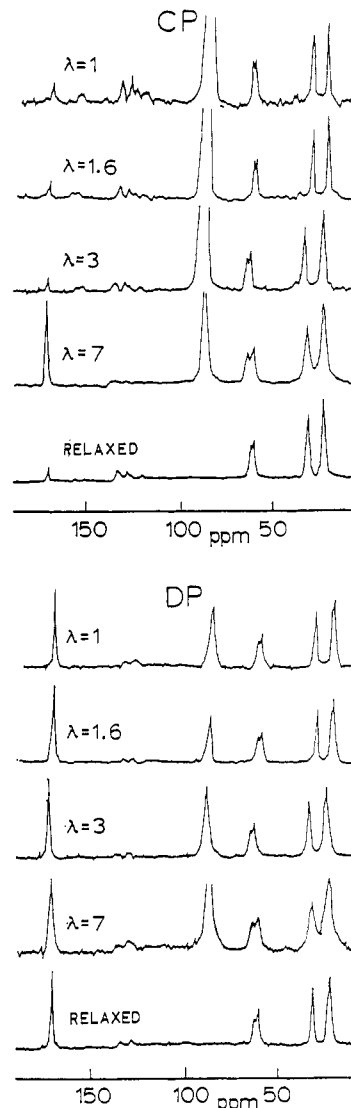


Figure 1. ^{13}C MAS-NMR spectra of a polyester-polyurethane elastomer at 50 MHz: (a, top) cross-polarization (CP time of 2 ms); (b, bottom) direct polarization (recycle delay of 3 s) for indicated extension.

Table I ^{13}C Chemical Shift of Polyester-Polyurethane	
	σ (ppm)
$-\text{O}-\overset{\text{O}}{\parallel}\text{C}-\text{CH}_2-\overset{*}{\text{CH}}_2-\overset{*}{\text{CH}}_2-\text{CH}_2-\overset{\text{O}}{\parallel}\text{C}-\text{O}$	24.2 ^a
$-\text{O}-\overset{*}{\text{CH}}_2-\overset{*}{\text{CH}}_2-\overset{*}{\text{CH}}_2-\text{CH}_2-\text{O}$	25.3 ^a
$-\text{O}-\overset{\text{O}}{\parallel}\text{C}-\overset{*}{\text{CH}}_2-\text{CH}_2-\text{CH}_2-\overset{*}{\text{CH}}_2-\overset{\text{O}}{\parallel}\text{C}-\text{O}$	33.3
$-\text{O}-\overset{*}{\text{CH}}_2-\overset{*}{\text{CH}}_2-\text{O}$	62.1 (60.8 for $\lambda = 7$)
$-\text{O}-\overset{*}{\text{CH}}_2-\text{CH}_2-\text{CH}_2-\overset{*}{\text{CH}}_2-\text{O}$	63.5
$-\text{CH}_2-\overset{*}{\text{C}}_6\text{H}_4-\overset{*}{\text{N}}\text{HCO}-$	110-140
$-\text{O}-\overset{\text{O}}{\parallel}\text{C}-(\text{CH}_2)_4-\overset{\text{O}}{\parallel}\text{C}-\text{O}$	172.7

^a Unresolved at $\lambda = 7$.

Cross-polarization dynamics was studied via plots of intensity versus spin lock time. Curves were fitted to the

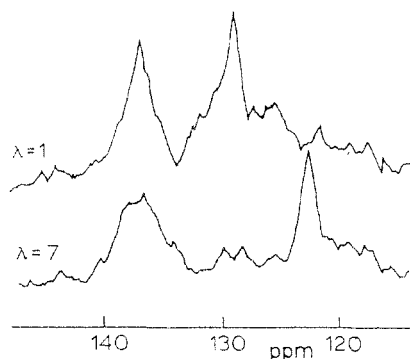


Figure 2. Expanded CP-MAS-NMR spectra for the aromatic carbons at $\lambda = 1$ and 7.

Table II
Second Moment of Polyester-Polyurethane of DP

extension (λ)	second moment (Hz)			
	$\text{CH}_2^*-\text{CH}_2-\text{CH}_2$	$\begin{array}{c} \text{O} \\ \\ -\text{C}-\text{CH}_2- \end{array}^*$	$-\text{O}-\text{CH}_2^--$	$\begin{array}{c} \text{O} \\ \\ -\text{C}- \\ * \end{array}$
1	270	210	270	1.3
1.6	260	216	270	1.3
3	310	260	325	1.3
7	570	505	614	2.4
relaxed	265	230	278	1.3

sum of two rising exponentials ($2 T_{\text{CH}}$) and a single $T_{1\rho}^{\text{H}}$ decay for multiple components of the well-understood cross-polarization mechanism.^{13,14} Each of the CP curves was fit by both a three-parameter (one rising and one falling exponential and a single intensity) equation and by a five-parameter (two rising exponentials and intensities and one falling exponential). For all but the $\lambda = 7$ case the sum of squares of the residuals for the five-parameter fit was 2.5–10-fold lower than that for the three-parameter fit. For the $\lambda = 7$ case the five-parameter sum of squares of residuals was only 20% lower but this sample had an intensity ratio of components of 10 to 1 so that the weak component would not make so much difference compared to a three-parameter fit. The results are listed in Table III with a typical set of data, and the fitting curve is shown in Figure 4. These T_{CH} values are plotted versus extension in Figure 5, showing that there are marked changes with extension indicating three components contributing to cross-polarization.

Discussion of Results

Because these are multicomponent materials with several possibilities for pure component phases, phase mixing, and interfacial states, they are difficult to describe simply and considerable ambiguity creeps into the interpretation of data from any one technique. For basic expectations of motional behavior the thermal transitions of the pure components should be kept in mind. Poly-(oxytetramethenyladipate) soft segments have glass and melting transitions at 155 and 321 K, respectively.^{15,16} One must bear in mind that, even though the observation temperature is below the crystallization temperature, the fraction of crystallinity will be low. This particular polyester soft segment was picked to enhance extensibility by virtue of the low fraction of crystallization. Thus for these segments in the pure state the expectations for the room-temperature measurements of this study are for moderate mobility. The chemical nature of the polyurethane segments is only inferred, but assuming it is made of ethylene glycol and MDI (vide infra) the 446 K glass¹⁷

and 512 K melting¹⁸ transitions are both very much greater than the NMR measurement temperature and thus pure polyurethane domains can be expected to be rigid glass and/or crystalline. One must regard this oversimplification of complete phase separation somewhat skeptically. Some of the urethane segments on topological grounds must be trapped adjacent to polyester (85 wt %) and are unable to form a glass or crystal, and phase mixing seems likely with such small domain sizes.

The relaxation times of Table III show much more dramatic changes with extension than do the spectra of Figure 1 and thus demonstrate the greater usefulness of relaxation studies over simple spectra for phase-separated systems of nonuniform morphology. Most dramatic in the case of Lycra 128 is the differentiation of soft-segment mobility regimes illustrated in Figure 5. Some important features emerge in the comparison of the spectra of samples at different extensions and in comparison of spectra at the same extension but obtained with CP or DP.

In the unextended sample the pronounced differences between CP and DP spectra are (1) the relative high intensity of the carbonyl carbon in the DP spectrum and (2) the observability of the aromatic peaks of the hard segments in the 110–140 ppm region only in the CP spectrum. These differences are readily explainable from examining the relaxation times of Table I and from the differing selectivity of the CP and DP observations. It must be realized that 87% of the carbonyls present are from the adipate segments. As only one chemical shift is observed, it must be assumed that only this adipoyl carbonyl is seen by NMR spectroscopy. The protons causing the carbonyl cross-polarization in the unextended sample are found to have $T_1^{\text{H}} = 0.26$ s, and the direct polarized carbonyl carbons have $T_1^{\text{C}} = 1.8$ s. This means that the carbonyl intensity in neither spectrum is limited by the recycle time. The CP intensity of the carbonyl for the fully extended sample is much greater than the intensities for the unextended and moderately extended samples. This loss of intensity reflects an inefficiency of the CP process due to relatively high mobility, as expected in the soft segments. The CH_2 peaks show no such dramatic loss of intensity, so this inefficiency must relate to the fact that cross-polarization is from distant nonbonded protons in the carbonyl case. T_1^{C} of the carbonyl spins prepared by the DP method yields $T_1^{\text{C}} = 1.9$ s, so it appears that CP and DP see the same carbons, but CP has a lower efficiency. DP observability is not limited so long as T_1^{C} is 5 times less than the recycle time, which we have done to avoid saturation. The aromatic urethane peaks at 110–140 ppm appear because they are rigid and thus cross-polarize efficiently. This demonstrates rigidity of the hard segments even in the unstretched sample. Because X-ray and DSC^{4,5} techniques have detected crystallinity, this rigidity is likely crystalline domains. The intensity of aromatics is at least 4 times lower in the DP spectrum because the CP enhancement factor is absent and possibly because the recycle time is short compared to the aromatic T_1^{C} . The intensity of these aromatic peaks was too low to allow determination of reliable relaxation times in a feasible amount of time.

The appearances of the CP and DP spectra do not change very dramatically with extension until extension is near ultimate. The small differences in resolution and line shape for moderately stretched samples will not be detailed here. The apparent weakening of the aromatic peaks in the CP spectra is not really a lowering of intensity but an intensifying of the peaks from the soft segments with extension. This can be seen in the relatively fewer scans

Table III
Relaxation Data^a of Polyester-Polyurethane

		carbon type			
		CH ₂ -CH ₂ -CH ₂	$\begin{array}{c} \text{O} \\ \\ -\text{C}-\text{CH}_2- \end{array}$	$\begin{array}{c} \text{O} \\ \\ -\text{O}-\text{CH}_2- \end{array}$	$\begin{array}{c} \text{O} \\ \\ -\text{C}- \\ * \end{array}$
T_1^H (s) CP	1	0.19	0.24	0.19	0.26
	1.6	0.24	0.26	0.21	0.35
	3	0.29	0.27	0.26	0.40
	7	0.59	0.71	0.65	0.59
	R ^b	0.30	0.32	0.32	0.44
$T_{1\rho}^H$ (ms) CP	1	9.9	9.1	8.7	19.9
	1.6	9.5	9.0	8.9	18.7
	3	10.1	8.9	9.0	20.7
	7	2.7	3.0	2.9	3.7
	R	9.6	9.6	9.2	20.4
T_1^C (s) DP	1	0.13	0.13	0.08	1.9
	1.6	0.13	0.13	0.08	1.9
	3	0.14	0.13	0.09	1.9
	7	0.23 (67%) 3.00 (33%)	0.29 (64%) 3.34 (36%)	0.26 (64%) 3.00 (36%)	4.9
	R	0.13	0.13	0.08	1.9
T_2^* (ms) DP	1	2.7	2.7	2.2	12.0
	1.6	2.7	2.7	2.0	12.0
	3	2.4	2.4	1.8	10.4
	7	0.02 (67%) 0.12 (33%)	0.01 (66%) 0.07 (34%)	0.02 (66%) 0.05 (33%)	
	R	2.5	2.5	2.0	12.0
T_2^* (ms) CP	1	2.0	2.0	1.7	3.3
	1.6	1.9	1.9	1.8	2.6
	3	1.9	1.9	1.7	3.0
	7	0.02 (71%) 0.10 (29%)	0.01 (74%) 0.08 (26%)	0.02 (71%) 0.05 (29%)	0.08 (54%) 0.40 (46%)
	R	2.0	1.8	2.2	3.3
T_{CH} (ms) ^c CP	1	2.4 ± 0.2 (60 ± 5%) 0.27 ± 0.02			
	1.6	2.4 ± 0.04 (54 ± 6%) 0.40 ± 0.01			
	3	2.8 ± 0.15 (77 ± 3%) 0.07 ± 0.004			
	7	0.8 ± 0.2 (11 ± 2%) 0.06 ± 0.01			
	R	0.73 ± 0.04 (96 ± 6%) ^d 0.07 ± 0.01			

^a Nominal 10% uncertainty on relaxation times except where designated otherwise. ^b R = sample at $\lambda = 7$ for 20 h and then relaxed. ^c Errors were estimated from the χ^2 surface as described in the Experimental Section. ^d The large error in this ratio results from the 6% error in the intensity of the minor component. Fitting without the minor component results in a 242% higher χ^2 , so there is no question that there is a minor component.

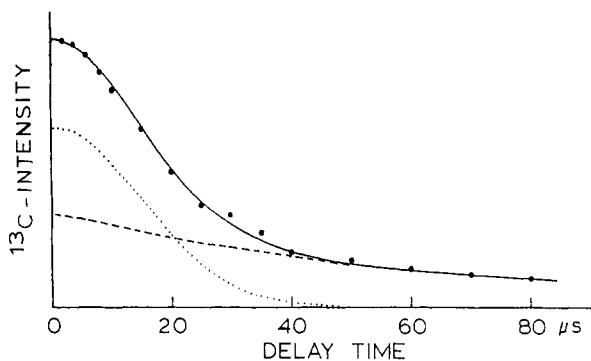


Figure 3. Dipolar dephasing of the ^{13}C MAS-NMR 33 ppm peak intensity as a function of delay time after DP pulses: (●) original data; (---) Lorentzian data; (---) Gaussian data; (—) sum of Lorentzian and Gaussian contributions. The recycle time was 15 s to allow for complete recovery to equilibrium of all species.

needed to acquire the spectra and is reflected in the improved noise figure, whereas the aromatic peaks are already at their maximum intensity in the unextended sample. Because the temperature of observation is only 20 K below T_m of the polyester, stretching could be inducing some crystalline domains or rigidity due to strain. These are difficult to distinguish.

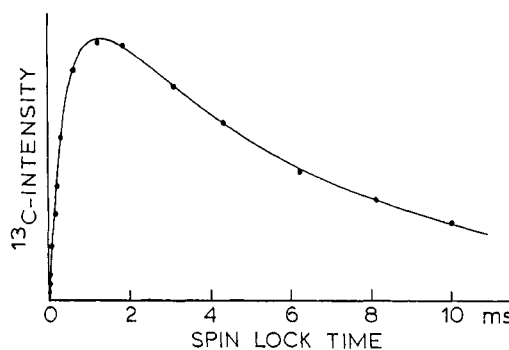


Figure 4. Carbon-13 intensity versus spin lock (cross-polarization) time for the 24 ppm CH_2 peak of the "relaxed" sample of Lycra 128 comparing data points (●) with the fitted curve for $T_{1\rho}^H = 10.56$ ms, $T_{CH}(a) = 0.73$ ms, $T_{CH}(b) = 0.073$ ms. Intensity a = 230 and intensity b = 10.9 as discussed in the text.

At near full extension of $\lambda = 7$ the carbonyl peak suddenly becomes very intense and there is a significant increase in the separation of the two peaks in the 62 ppm region. The dramatic carbonyl increase based on the above discussion is undoubtedly due to increased rigidity of the protons near the carbonyl. The shift in apparent resolution in the 62 ppm region is due to the shift of the peaks assigned to $\text{OCH}_2\text{CH}_2\text{O}$ carbons from 62.1 ppm in the unextended

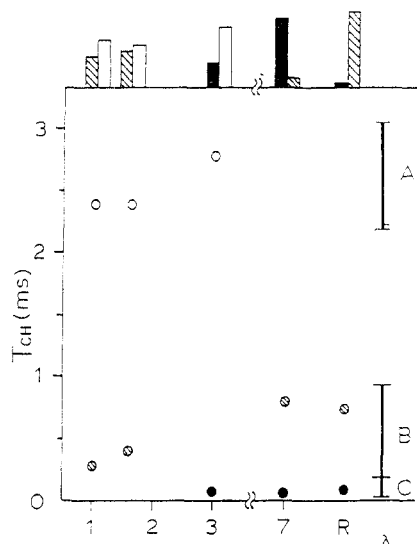


Figure 5. Plot of T_{CH} versus extension for Lycra 128 sample. The graph is divided into three domains for different levels of restriction of the segments as elaborated in the text.

sample to 60.8 ppm at $\lambda = 7$. This upfield shift could be the result of increased population of the trans conformers or could be due to packing effects in crystallites. Examination of the literature is not conclusively helpful. Polyethylene gives an approximate 2 ppm downfield shift on going from amorphous to crystalline form, which is explained on the basis of a gauche-to-trans conformational change.¹⁹ Poly(oxyethylene), which is perhaps a better model for the case at hand, shows a shift upfield for the amorphous-to-crystalline transition.²⁰ However, a dipolar dephasing study in poly(ethylene oxide) gives no chemical shift difference between crystalline and noncrystalline components of a semicrystalline sample.²¹

It is of interest that the CP spectrum of the "relaxed" sample does not completely revert to the spectrum of the unstretched state even after several days. This must mean that there is irreversible change generated in the stretching of the material. This is certainly in agreement with the large hysteresis seen in Lycra extension/DSC studies.²² The spectra of the DP-detectable carbons show no difference between the relaxed and unstretched material presumably because in the amorphous state the chains all have similar motional properties; on the other hand in the crystalline, CP-detected material, relaxation and line shape properties are a strong function of crystal size and spin exchange with other domains of the sample.¹⁹

The change in line shape with extension in the 120–140 ppm aromatic region is experimentally unambiguous. Even though the signal to noise ratio is poor, it is clear that the peaks at 129 ppm and 137–8 ppm diminish in intensity with increasing extension. These peaks are assignable easily to the protonated and unprotonated aromatic carbons, respectively. In the $\lambda = 7$ sample a new peak appears at 122 ppm, the 129 ppm all but disappears, and the 137–8 ppm peaks broadens. The nature of the magic angle spinning experiment dictates that the chemical shift and dipolar tensors average to the isotropic chemical shift and zero, respectively, for the exact magic angle. The tuning procedures in our laboratory adjust the magic angle on an aromatic sample so that averaged chemical shift anisotropy is less than the 2 ppm line width. Thus this phenomenon of change in aromatic line shapes even to the point of disappearance and appearance of lines is quite peculiar. A reasonable speculation is that relaxation times of the rather highly oriented material, the $\lambda = 7$ case, are anisotropically affected by the modulation of the dipolar

field through spinning, broadening some peaks, and narrowing others.

Because the peaks were not all resolved and the line width differences were subtle, we chose to analyze the shape changes of the four main peaks in the CP spectrum as second moments of the shapes. The results tabulated (Table II) show some changes in the line shape with extension, with a dramatic change near the extreme extension. Curiously, only two of the peaks revert back to the unstretched parameter on relaxation. This may indicate that a small population of the OC^*H_2 and $O=CC^*H_2$ carbons is entrapped in the permanent strain-induced immobilization.

As a further step in characterizing the changes in the samples with extension, we measured the rate of decay of the transverse ^{13}C signal with delay in a dipolar dephasing experiment. For all but the $\lambda = 7$ sample the decay was Lorentzian. For the $\lambda = 7$ sample the intensity versus delay profiles are typified by Figure 3. The profile was analyzed as a sum of Gaussian and Lorentzian components

$$M(t) = M_{0,g} \exp[-0.5(t/T_{2g}^*)^2] + M_{0,l} \exp(-t/T_{2l}^*) \quad (1)$$

where $M(t)$ is the carbon intensity at any time. $M_{0,g}$ and $M_{0,l}$ are, respectively, the Gaussian and Lorentzian components at $t = 0$ which decay with the characteristic decay times T_{2g}^* and T_{2l}^* . Because of the intensity differences between CP and DP spin preparations, particularly for the carbonyl resonance, the dipolar dephasing analysis was done for both methods and the resulting T_2^* values are tabulated in Table III along with the fractional contribution of each component to the $t = 0$ intercept. The observation that T_2^* is found to be essentially the same for the DP and CP cases (except for the carbonyl) means that we are observing the same carbon populations in both methods. For the unstretched sample the carbonyl resonance shows a T_2^* about 4-fold longer in the DP case compared to the CP case, so in this instance different carbonyls were probably sampled by the two techniques. In both DP and CP for the CH_2 segments there is only a slight decrease in T_2^* with extension until the $\lambda = 7$ sample. In this case two T_2^* are observed which are both over 1 order of magnitude shorter than the T_2^* at lower extension. The assignment of the fast Gaussian and slower Lorentzian relaxations to physical states is somewhat speculative, but a reasonable assertion can be made. Certainly, these two components ($T_2^* = 0.1$ and 0.02 ms) at $\lambda = 7$ extension represent states quite different from those found at low extension ($T_2^* = 2.5$ ms). The DSC and x-ray results^{4,5} show the existence of crystallinity which would be commensurate with very strong dipolar interactions, i.e. very short T_2^* of the Gaussian component. The Gaussian decay of this component may result from strong dipolar interactions only partially averaged in the sense of the van Vleck dipolar line shape and from partial averaging of the second moment.²³ The other relatively short T_2^* must belong to some state which is more restricted than the unstretched material but not crystalline. It is not unreasonable to assign this to "strained" segments.

Given the analysis of the cross-polarization dynamics in Figures 4 and 5, it seems possible to explain the effects of extension on the soft segments. The relationship of mobility and T_{CH} is well understood.^{14,24} We find three clear ranges of T_{CH} values in these extended samples, as shown in Figure 5. In the unextended material there is a long 2.4-ms and a medium 0.27-ms relaxation time. For a CH_2 group the long value is typical for mobile bulk segmental motion above T_g ²⁵ and so we assign it to "bulk" mobility. Clearly, the dominant species, having very short

value of 0.07 ms in the fully extended sample must belong to the crystalline phase, as discussed above for the shortest T_2^* value. This leaves the midrange values 0.1–0.75 ms to be assigned. This value is remarkably shorter than the bulk value. The value of T_{CH} lengthens with increased mobility, so qualitatively this must be a relatively rigid material but one which is not truly crystalline. We assign this to chains with restricted or strained chain motion, i.e. fewer available "conformation sites" than a purely random chain.

This NMR result is in conflict with previous analyses in the sense that the commonly discussed "strain induced crystallinity of the soft segments"^{1,4} appears not be crystallinity at all until the polymer is fully extended for this polyester-polyurethane. These results are also in disagreement with Bonart's model² which suggests loss of crystallinity of soft segments with extension. There may be a gradual increase in crystallinity, but the exclusive selectivity of DSC and X-ray methods for crystalline domains may have caused undue weighing of the crystalline domains in explaining the increases of modulus with extension. NMR spectroscopy is shown in this application to be capable of weighing all of the material present.

The observation that T_1^H changes gradually with extension whereas $T_{1\rho}^H$ does not is an interesting one (both relaxation times are measured on the CP-prepared spins). The latter parameter is a much more local one because it is on the order of milliseconds. There is less time for spin diffusion to "equalize" the relaxation times from all domains in the sample as compared to the T_1^H case.⁹ In light of the sharp drop in both relaxation times at full extension, there should certainly be a different contribution from the bulk, restricted, or crystalline domains. However, $T_{1\rho}^H$ is measured after a CP spin preparation so by this selection less mobile domains are observed, as evidenced by the CP dynamics showing 89% fast component (Table III). As this relaxation time is only milliseconds, these rigid domains are not strongly influenced via spin diffusion by the more relaxed domains. The longer T_1^H , tenths of seconds, allows this spin diffusion to "average" over a larger distance, perhaps a 1000-Å scale. Thus the net value of T_1^H shows the weighted influence of all domains, the relative amount of each domain changing with extension. A quantitative analysis of the relative contribution of the more-rigid and less-rigid domains which yields the observed relaxation times would be a difficult task. It would require methods which would give exact descriptions of the rate of spin diffusion. Further problems, especially at high extension would arise from separating dipolar and motional parts of $T_{1\rho}^H$.²⁶ However, the discussion above on cross-polarization dynamics, because T_{CH} is in many cases very short, offers some real hope on quantitative separation of domains.

Summary

Overall, these results show that MAS-NMR spectroscopy adds rich detail to the description of the effects of

extension on elastomers. Although these segmented polyester-polyurethanes are highly complex, semicrystalline, multiphase systems, we have made measurements on the constituent hard and soft segments and distinguished three motional regimes of the latter. There is little soft segment crystallinity even at modest extension. Near ultimate extension 90% of the soft segments are very rigid, presumably crystalline. Relaxation of stress does not restore the original "bulk" mobility of the virgin sample.

References and Notes

- (1) Finelli, A. F.; Marshall, R. A.; Chuang, D. A. In *Encyclopedia of Chemical Technology*; Grayson, M., Ed.; J. Wiley: New York, 1979; p 632.
- (2) Bonart, R. J. *Macromol. Sci.-Phys* **1986**, B2 (1), 115.
- (3) Seymour, R. W.; Cooper, S. L. *Macromolecules* **1973**, 6, 48.
- (4) Wang, D.; Lyon, R. E.; Farris, R. J. *Chin. J. Polym. Sci.* **1987**, 3, 262.
- (5) Wang, D.; Lyon, R. E.; Farris, R. J. *Chin. J. Polym. Sci.* **1987**, 3, 274.
- (6) Dickinson, L. C.; Shi, J.-F.; Chien, J. C. W. *Macromolecules* **1992**, 25, 1224.
- (7) M. Alla; Lippaa, E. *Chem. Phys. Lett.* **1976**, 37, 260.
- (8) Torchia, D. J. *Magn. Reson.* **1978**, 30, 612.
- (9) Schaefer, J.; Stejskal, E. O.; Buchdahl, R. *Macromolecules* **1975**, 8, 291.
- (10) Dickinson, L. C.; Yang, H.; Chu, C.-W.; Stein, R. S.; Chien, J. C. W. *Macromolecules* **1987**, 20, 1757.
- (11) Bevington, P. R. *Data Reduction and Error Analysis for the Physical Sciences*; McGraw Hill: New York, 1969.
- (12) Abragam, A. *Principles of Nuclear Magnetism*; Oxford University Press: Oxford, U.K., 1962; p 106.
- (13) Huigen, T. P.; Gaur, H. A.; Weeding, T. L.; Jenneskens, L. W.; Schuur, H. E. C.; Hyssmans, W. G. B.; Veeman, W. S. *Macromolecules* **1990**, 23, 3063.
- (14) Pines, A.; Gibby, M. G.; Waugh, J. S. *J. Phys. Chem.* **1973**, 59, 569.
- (15) Grieseson, B. M. *Polymer* **1980**, 1, 488.
- (16) Zilberman, E. N.; Kulikova, A. E.; Teplyakov, N. M. *J. Polym. Sci.* **1962**, 56, 417.
- (17) MacKnight, W. J.; Yang, M.; Kajiyama, T. *ACS Polym. Prepr.* **1968**, 9, 860.
- (18) Lyman, D. J.; Heller, J.; Barlow, M. *Makromol. Chem.* **1965**, 84, 64.
- (19) Axelsson, D. E. In *High Resolution NMR Spectroscopy of Synthetic Polymers in Bulk*; Komoroski, R. A., Ed.; VCH Publishers: Deerfield Beach, FL, 1986; p 226.
- (20) Cholli, A. L.; Ritchey, W. M.; Koenig, J. L. *Spectrosc. Lett.* **1983**, 16, 21.
- (21) Axelsson, D. E. In *High Resolution NMR Spectroscopy of Synthetic Polymers in Bulk*; Komoroski, R. A., Ed.; VCH Publishers: Deerfield Beach, FL, 1986; p 220.
- (22) Moritzer, L.; Hespe, H. J. *Appl. Polym. Sci.* **1972**, 16, 2097.
- (23) Abragam, A. *Principles of Nuclear Magnetism*; Oxford University Press: Oxford, U.K. 1962; pp 432–435.
- (24) Pines, A.; Gibby, M. G.; Waugh, J. S. *Chem. Phys. Lett.* **1972**, 15, 373.
- (25) Laupretre, F.; Monnerie, L.; Virlet, J. *Macromolecules* **1984**, 17, 1397.
- (26) Stejskal, E. O.; Schaefer, J.; Sefcik, M. D.; McKay, R. A. *Macromolecules* **1981**, 14, 275.

Registry No. MDI/HO₂C(CH₂)₄CO₂H/HO(CH₂)₄OH/HO(CH₂)₂OH (copolymer), 26375-23-5.